Inorg. Chem. **2007**, *46*, 2362–2364

A Rh^{II}–Au^{II} Bimetallic Core with a Direct Metal–Metal Bond

Arthur J. Esswein, Jillian L. Dempsey, and Daniel G. Nocera*

Department of Chemistry, Massachusetts Institute of Technology, Building 6, Room 335, 77 Massachusetts Avenue, Cambridge, Massachusetts 02139-4307

Received November 19, 2006

The $d^8\cdots d^{10}$ heterobimetallic $Rh^IAu^I(tfepma)_2(CN^tBu)_2Cl_2$ (**1**) complex (tfepma = bis[bis(trifluoroethoxy)phosphino]methylamine) is oxidized by $KAu^{III}Cl_4$ to give the first structurally characterized d^7–d^9 Rh^{II}–Au^{II} singly bonded metal complex $[Rh^{II}Au^{II}(tfepma)_2(CN^tBu)_2Cl_3]^+[Au^ICl_2]^-$ (**2**). Complex **2** undergoes a thermal intermetal redox reaction to generate *fac*-$Rh^{III}(tfepma)(CN^tBu)Cl_3$ (**3**) and $Au_2^{I,I}(tfepma)_2Cl_2$ (**4**).

Bimetallic Rh complexes bridged by three dfpma ligands [dfpma = $CH_3N(PF_2)_2$] are photocatalysts for hydrogen production from homogeneous HX solutions.[1] Reactivity studies suggest that 2 equiv of HX add to a $Rh_2^{0,0}$ center to generate a dihydridodihalo $Rh_2^{II,II}(H)_2(X)_2$ complex from which H_2 is photoeliminated.[2] The Rh^{II}–X bond of the resulting dihalide $Rh_2^{0,II}(X)_2$ photoproduct may be activated by excitation into the $d\sigma \rightarrow d\sigma^*$ absorption manifold[3] of the bimetallic core to give back the $Rh_2^{0,0}$ center, thus closing the photocycle.[4,5] Rh^{II}–X bond activation is the overall determinant of the photocycle efficiency and consequently the efficiency of H_2 production.[2] One way to increase the photocycle efficiency is to increase the photochemical quantum yield for M–X bond activation. Gold halide complexes are light-sensitive and thus are attractive targets for photochemical studies.[6] To this end, we have begun to develop a chemistry of heterobimetallic RhAu complexes with the objective of managing H_2 at the Rh end and X_2 at Au end of the bimetallic core. The majority of RhAu heterobimetallics to date have employed either dppm [bis(diphenylphosphino)methane] or dcpm [bis(dicyclohexylphosphino)methane] as bridging ligands. Of pertinence to the chemistry reported here, $Rh^IAu^I(dppm)_2(CN^tBu)_2Cl_2$ was first synthesized by Langrick and Shaw[7] and recently characterized by X-ray crystallography.[8] Though the compound has been the subject of spectroscopic investigations,[9–11] the reaction chemistry of $Rh^I\cdots Au^I$ and more generally $d^8\cdots d^{10}$ cores has been underdeveloped. We now report the synthesis, characterization, and redox chemistry of a $Rh^I\cdots Au^I$ complex to generate a two-electron oxidized Rh^{II}–Au^{II} complex, which contains a formal metal–metal bond.

$Rh^IAu^I(tfepma)_2(CN^tBu)_2Cl_2$ (**1**) can be synthesized by the sequential addition of tfepma [tfepma = $CH_3N(P[OCH_2CF_3]_2]$, *tert*-butylisonitrile, and $Au^I(tht)Cl$ (tht = tetrahydrothiophene) to a concentrated solution of $[Rh^I(COD)Cl]_2$ in CH_2Cl_2 in 83% yield. The NMR spectrum of **1** in CD_3CN shows a sharp singlet at 1.45 ppm for the *tert*-butyl protons of the terminal isonitriles and a pseudotriplet at 2.98 ppm ($^3J_{P-H}$ = 3.0 Hz) for the bridgehead *N*-methyl protons. $^{31}P\{^1H\}$ NMR shows two multiplets at 136.9 and 151.3 ppm. Single crystals of **1** may be obtained from CH_2Cl_2 solutions of the complex layered with Et_2O. The solution of the X-ray crystal structure is shown in Figure 1 (left). The ligand geometries about the Rh and Au centers are in accordance with that expected for their respective d electron counts. The Rh^I center is approximately square-planar, and the Au^I center is trigonally distorted as defined by P(1)–Au(1)–P(2) and P(1)–Au(1)–Cl(1) angles of 151.41(3)° and 101.39(3)°, respectively. The chloride counterions show close metal contacts of d[Au(1)···Cl(1)] = 2.6632(9) Å and d[Rh(1)···Cl(2)] = 2.6027(9) Å. The Rh(1)···Au(1) distance is 2.8181(3) Å. The structural motif of **1** is similar to that of other $d^8\cdots d^{10}$ M···Au^I dimers (M = Rh^I,[8] Ir^I,[12] Ni^{II},[13] Pt^{II} [14]) when dppm and dcpm bridging ligands are used, except that the

* To whom correspondence should be addressed. E-mail: nocera@mit.edu.

(1) Heyduk, A. F.; Nocera, D. G. *Science* **2001**, *293*, 1639–1641.
(2) Esswein, A. J.; Veige, A. S.; Nocera, D. G. *J. Am. Chem. Soc.* **2005**, *127*, 16641–16651.
(3) Kadis, J.; Shin, Y.-g. K.; Ward, D. L.; Nocera, D. G. *Inorg. Chem.* **1996**, *35*, 811–817.
(4) Heyduk, A. F.; Macintosh, A. M.; Nocera, D. G. *J. Am. Chem. Soc.* **1999**, *121*, 5023–5032.
(5) Odom, A. L.; Heyduk, A. F.; Nocera, D. G. *Inorg. Chim. Acta* **2000**, *297*, 330–337.
(6) See: Fackler, J. P., Jr. *Inorg. Chem.* **2002**, *41*, 6959–6972.
(7) Langrick, C. R.; Shaw, B. L. *J. Chem. Soc., Dalton Trans.* **1985**, 511–516.
(8) Dempsey, J. L.; Esswein, A. J.; Manke, D. R.; Rosenthal, J.; Soper, J. D.; Nocera, D. G. *Inorg. Chem.* **2005**, *44*, 6879–6892.
(9) Striplin, D. R.; Crosby, G. A. *J. Phys. Chem.* **1995**, *99*, 7977–7984.
(10) Striplin, D. R.; Crosby, G. A. *J. Phys. Chem.* **1995**, *99*, 11041–11045.
(11) Yip, H.-K.; Lin, H.-M.; Wang, Y.; Che, C.-M. *Inorg. Chem.* **1993**, *32*, 3402–3407.
(12) For crystallographically characterized $Ir^I\cdots Au^I$ complexes, see: (a) Balch, A. L.; Catalano, V. J.; Olmstead, M. M. *Inorg. Chem.* **1990**, *29*, 585–586. (b) Balch, A. L.; Catalano, V. J. *Inorg. Chem.* **1991**, *30*, 1302–1308.
(13) For a crystallographically characterized $Ni^{II}\cdots Au^I$ complex, see: Kim, H. P.; Fanwick, P. E.; Kubiak, C. P. *J. Organomet. Chem.* **1988**, *346*, C39–C42.

10.1021/ic062203f CCC: $37.00
Published on Web 02/28/2007

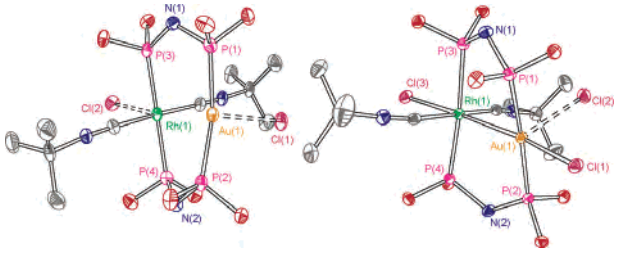

Figure 1. Ellipsoid plots of **1** (left) and **2** (right). H atoms, noncoordinating counterions, and −Me and $-CH_2CF_3$ groups are omitted for clarity. Data collected at 100 K with thermal ellipsoids drawn at the 50% probability level.

Scheme 1

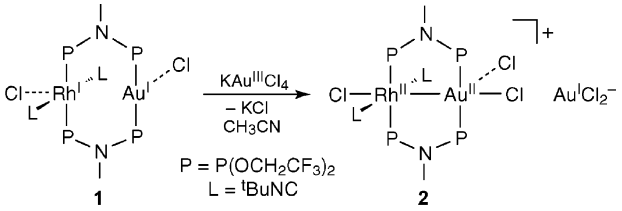

closely associated chlorides dispose the Au^I center toward a trigonal geometry in lieu of the nearly linear geometry observed in other systems.[8,12−14]

The highest occupied molecular orbital (HOMO) of $d^8\cdots d^{10}$ bimetallic centers, as is the case for the $Rh^I\cdots Au^I$ complex, is a highly destabilized and occupied dσ* orbital arising from a $d_{z^2}-d_{z^2}$ interaction.[9−11,15] Notwithstanding, oxidation of **1** with outer-sphere one-electron oxidants such as NO^+ and $R_3N^{\bullet+}$ gives intractable product mixtures. Similar results are obtained for $PhI\cdot Cl_2$, which is an oxidant and chlorine delivery agent. Conversely, a prompt color change from orange to red is observed upon the addition of $KAu^{III}Cl_4$ to CH_3CN solutions of **1** at low temperature (Scheme 1). A UV−vis absorption spectrum of the reaction mixture confirms that the conversion proceeds smoothly. The diagnostic absorption bands of **1** at 380 and 421 nm, which are in line with those reported for a RhAu dσ* → CNR π*/RhAu pσ transition,[11] are replaced by two new absorption bands at 329 and 460 nm (Figure 2).

Oxidation product **2** may be isolated as a strawberry solid in 44% yield after removal of KCl and subsequent recrystallization from CH_2Cl_2 layered with pentane. The NMR signals of **2** are significantly shifted from those of **1**. A ^1H NMR singlet for the equivalent *tert*-butyl protons is observed at 1.61 ppm and a pseudotriplet ($^3J_{P-H} = 4.4$ Hz) is observed for the bridgehead N−Me groups at 3.05 ppm. The $-OCH_2CF_3$ protons appear as a series of complex multiplets at

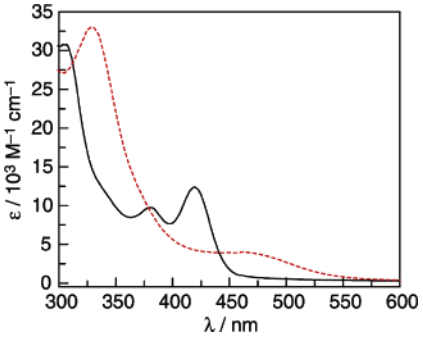

Figure 2. UV−vis absorption spectra from 300 to 600 nm (25 °C, CH_3CN) for **1** (—) and immediately after the addition of 1.05 equiv of $KAu^{III}Cl_4$ to generate **2** (- - -).

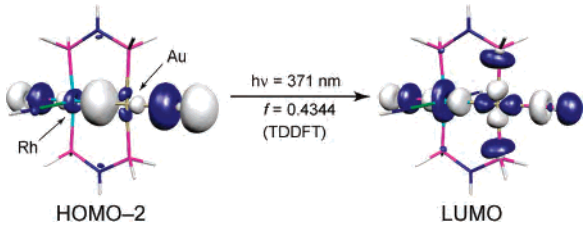

Figure 3. DFT calculation of the orbitals involved in the dσ → dσ* transition of $Rh^{II}Au^{II}(HN[PH_2]_2)_2(CNH)_2Cl_2^{2+}$. Geometry optimization was initiated using coordinates obtained from the crystal structure of **2**. Oscillator strengths and transition energies were calculated by time-dependent DFT.

~4.65, 4.99, and 5.79 ppm. The $^{31}P\{^1H\}$ NMR spectrum of **2** indicates a large structural deviation from **1** as the two distinct ^{31}P NMR resonances of **1** at 136.9 and 151.3 ppm are lost and replaced by a complex set of overlapping multiplets centered at ~98 ppm. Single-crystal X-ray diffraction studies of **2** unequivocally establish its identity as $[Rh^{II}Au^{II}(tfepma)_2(CN^tBu)_2Cl_3]^+[Au^ICl_2]^-$ (Figure 1, right); the Rh^{II} center is pseudooctahedral, and the Au^{II} center is roughly square-planar. Metal−halide bonding interactions are reflected by Rh(1)−Cl(3) and Au(1)−Cl(1) distances of 2.3764(9) and 2.4267(8) Å, respectively. Additionally, the short Rh(1)−Au(1) distance of 2.6549(4) Å in **2** is indicative of a formal metal−metal bond, thus affording the first structural characterization of a $Rh^{II}-Au^{II}$ interaction.[16] A chloride ion is loosely associated at an apical position of the Au^{II} square plane at a contact distance of 2.8492(9) Å. The cationic complex is charge-balanced by an outer-sphere $Au^ICl_2^-$ counterion.

Density functional theory (DFT) calculations were initiated using the coordinates obtained from the crystal structure of **2** (see the Supporting Information, SI). H atom surrogates were used in place of −Me, $-^tBu$, and $-OCH_2CF_3$ groups. The agreement between calculated and observed structures suggests that these simplifications are reasonable. Details of the computation are provided in the SI. Time-dependent DFT calculations identify an allowed singlet dσ → dσ* transition between the HOMO−2 and lowest unoccupied molecular orbital, which is shown in Figure 3. This result is consistent with a d^7-d^9 electron count, which can also be described as

(14) For crystallographically characterized $Pt^{II}\cdots Au^I$ complexes, see: (a) Manojlović-Muir, L.; Henderson, A. N.; Treurnicht, I.; Puddephatt, R. J. *Organometallics* **1989**, *8*, 2055−2061. (b) Yip, H.-K.; Che, C.-M.; Peng, S.-M. *J. Chem. Soc., Chem. Commun.* **1991**, 1626−1628. (c) Yip, H.-K.; Lin, H.-M.; Wang, Y.; Che, C.-M. *J. Chem. Soc., Dalton Trans.* **1993**, 2939−2944. (d) Xu, C.; Anderson, G. K.; Brammer, L.; Braddock-Wilking, J.; Rath, N. P. *Organometallics* **1996**, *15*, 3972−3979. (e) Xia, B.-H.; Zhang, H.-X.; Che, C.-M.; Leung, K.-H.; Phillips, D. L.; Zhu, N.; Zhou, Z.-Y. *J. Am. Chem. Soc.* **2003**, *125*, 10362−10374.

(15) Also by analogy to homobimetallic $d^8\cdots d^8$ systems, see for example: (a) Rice, S. F.; Miskowski, V. M.; Gray, H. B. *Inorg. Chem.* **1988**, *27*, 4704−4708. (b) Roundhill, D. M.; Gray, H. B.; Che, C.-M. *Acc. Chem. Res.* **1989**, *22*, 55−61.

(16) As determined from a search of the Cambridge Structural Database. No matches were obtained for direct Rh−Au linkages in these formal oxidation states.

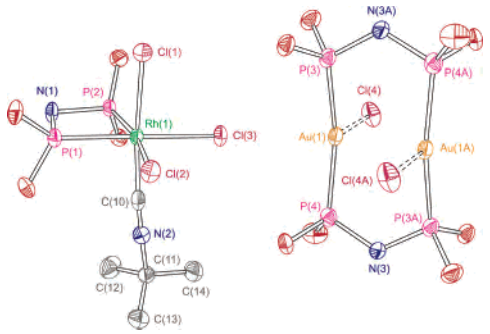

Figure 4. Ellipsoid plots of the cocrystallized products **3** (left) and **4** (right) when solutions of **2** were left to stand at room temperature in CH_3CN. H atoms and $-$Me and $-CH_2CF_3$ groups are omitted for clarity. Data collected at 100 K with thermal ellipsoids drawn at the 50% probability level.

$(d^6)d^1-(d^8)d^1$, where the odd electron on each of the individual metal centers resides in a d_{z^2} orbital.[4]

Butyronitrile glasses (77 K) of **1** display a weak emission band at 565 nm and a strong band at 707 nm ($\lambda_{exc} = 420$ nm), with lifetimes of <10 ns and 20 μs indicating an excited-state parentage that is singlet and triplet, respectively,[9,10] or indicating intermolecular association (for the short-lifetime component) of a bimetallic containing Au.[17] Complex **2** is also emissive at 77 K and displays two bands at 529 and 733 nm. As in **1**, the red band is assigned as phosphorescence based on the observed lifetime of 30 μs. The low-energy phosphorescence is consistent with emission from dσ* excited states, as is observed for bimetallic Rh cores.[3] The lifetime of the emissive state centered at 529 nm was <10 ns.

At ambient temperatures, complex **2** is unstable in solution and thermally reacts in CH_3CN or CH_2Cl_2 over the course of several hours. The complex multiplet centered at ~98 ppm in the $^{31}P\{^1H\}$ NMR spectrum of **2** disappears with the concomitant appearance of a singlet resonance at 134.4 ppm and a sharp doublet at 75.5 ppm with a $^1J_{Rh-P}$ coupling constant of 141.9 Hz, in a 1:1 ratio. Although the ^1H NMR spectrum contains multiple overlapping N$-$Me resonances, a ^{t}BuNC resonance appears at 1.56 ppm, consistent with the formation of $Au^I(CN^tBu)Cl$.[18]

Direct evidence for cleavage of the heterobimetallic $Rh^{II}-Au^{II}$ bond is provided by single crystals obtained from CH_2Cl_2/pentane layers of reacted solutions. X-ray structural analysis showed the asymmetric unit to contain *fac*-Rh^{III}(t-fepma)$(CN^tBu)Cl_3$ (**3**) and $Au_2^{I,I}(tfepma)_2Cl_2$ (**4**) (Figure 4), tentatively assigned as the resonances at 75.5 and 134.4 ppm, respectively, in the $^{31}P\{^1H\}$ NMR. The structure of **3** comprises a pseudooctahedral Rh^{III} center ligated by three chloride ligands in a facial geometry with ~90° cis angles and typical Rh$-$Cl bond lengths of 2.37$-$2.41 Å. A single CN^tBu ligand is coordinated trans to Cl(1) with a linear Cl(1)$-$Rh(1)$-$C(10) angle of 174.00(18)°. The largest deviation from an ideal octahedral geometry is the tight P(1)$-$Rh(1)$-$P(2) bite angle of 70.94(6)° that is imposed by the chelating tfepma ligand. The overall structural motif is analogous to that observed in *fac*-$Rh^{III}(dppm)(CH_3CN)Cl_3$.[19] Complex **4** sits on a special position in the crystal lattice, and the bimetallic core is bisected by a crystallographic inversion center. The coordination geometry about the Au center in **4** is analogous to that of **1** with similar Au$-$P distances of 2.2973(18) and 2.2878(17) Å; the Au(1)$\cdots$Cl(4) contact is long at 2.6364(16) Å. The distorted trigonal geometry is defined by P(3)$-$Au(1)$-$P(4) and P(3)$-$Au(1)$-$Cl(4) angles of 159.40(6)° and 98.00(6)°, respectively. The tfepma ligand engenders an Au(1)$\cdots$Au(1A) distance of 2.8390(5) Å. This intermetal distance is shorter by about ~0.1 Å with respect to Au dimers of similar formulations with bridging dppm or dcpm ligands.[20,21]

The thermal reaction of **2** to yield **3** and **4** indicates that the $Rh^{II}-Au^{II}$ metal$-$metal-bonded core is eradicated by intermetal charge transfer and disproportionation by the overall stoichiometry: $\mathbf{2} \rightarrow \mathbf{3} + {}^1/_2\mathbf{4} + Au^I(CN^tBu)Cl$. It is not unreasonable, on the basis of electronegativity differences, to invoke a bonding interaction between the d^7 Rh^{II} and d^9 Au^{II} centers that is highly polarized toward Au; in this instance, a $d^6 \leftarrow d^{10}$ electron count for a $Rh^{III} \leftarrow Au^I$ interaction is the limiting oxidation state formalism. If this electronic contribution was significant, then the high-valent Rh^{III} center would be expected to expel neutral π-acceptor ligands in lieu of anionic π-donor ligands such as Cl^-. In light of this possibility, further investigations on the two-electron redox chemistry of $d^8\cdots d^{10}$ cores may be facilitated by replacing the group 9 metal center with one from group 10.[14,22,23] The d orbital energies for Pt and Au metal fragments are expected to be better matched, leading to more covalent M$-$M interactions, which could aid in the stabilization of the $Pt^{III}-Au^{II}$-bonded d^7-d^9 core and avoid the disproportionation chemistry observed for $Rh^{II}-Au^{II}$ cores. The elaboration of such compounds is currently under investigation.

Acknowledgment. This research was supported by grants from the NSF (Grant CHE-0132680). J.L.D. acknowledges support from the UROP office at Massachusetts Institute of Technology (MIT). Grants from the NSF also provided instrument support to the DCIF at MIT (Grants CHE-9808061 and DBI-9729592) and for X-ray diffraction facilities under the auspices of a MRSEC Program (Grant DMR 02-13282).

Supporting Information Available: Computational, crystallographic (CIF), and full experimental procedures. This material is available free of charge via the Internet at http://pubs.acs.org.

IC062203F

(17) For example, see: van Zyl, W. E.; Lopez-de-Luzuriaga, J. M.; Mohamed, A. A.; Staples, R. J.; Fackler, J. P., Jr. *Inorg. Chem.* **2002**, *41*, 4579$-$4589.
(18) Liau, R.-L.; Mathieson, T.; Schier, A.; Berger, R. J. F.; Runeberg, N.; Schmidbaur, H. *Z. Naturforsch. B* **2002**, *57*, 881$-$889.
(19) Cotton, F. A.; Dunbar, K. R.; Eagle, C. T.; Falvello, L. R.; Kang, S.-J.; Price, A. C.; Verbruggen, M. G. *Inorg. Chim. Acta* **1991**, *184*, 35$-$42.
(20) Schmidbaur, H.; Wohlleben, A.; Schubert, U.; Frank, A.; Huttner, G. *Chem. Ber.* **1977**, *110*, 2751$-$2757.
(21) Fu, W.-F.; Chan, K.-C.; Cheung, K.-K.; Che, C.-M. *Chem. Eur. J.* **2001**, *7*, 4656$-$4664.
(22) Cooper, G. R.; Hutton, A. T.; Langrick, C. R.; McEwan, D. M.; Pringle, P. G.; Shaw, B. L. *J. Chem. Soc., Dalton Trans.* **1984**, 855$-$862.
(23) Hassan, F. S. M.; Markham, D. P.; Pringle, P. G.; Shaw, B. L. *J. Chem. Soc., Dalton Trans.* **1985**, 279$-$283.